Cytokine 118 (2019) 130–143

Contents lists available at ScienceDirect

Cytokine

journal homepage: www.elsevier.com/locate/cytokine

M2 polarization of macrophages by Oncostatin M in hypoxic tumor microenvironment is mediated by mTORC2 and promotes tumor growth and metastasis

Richa Shrivastava[a,b], Mohammad Asif[a], Varsha Singh[a], Parul Dubey[c], Showkat Ahmad Malik[a], Mehraj-U-Din Lone[a], Brij Nath Tewari[c], Khemraj Singh Baghel[a], Subhashis Pal[d], Geet Kumar Nagar[d], Naibedya Chattopadhyay[d], Smrati Bhadauria[a,b,*]

[a] Division of Toxicology and Experimental Medicine, Central Drug Research Institute (CSIR), Lucknow, Uttar Pradesh 226031, India
[b] Academy of Scientific and Innovative Research (AcSIR), New Delhi 110025, India
[c] Department of Surgical Oncology, King George Medical University, Lucknow, Uttar Pradesh 226003, India
[d] Division of Endocrinology and Centre for Research in Anabolic Skeletal Target in Health and Illness (ASTHI), Central Drug Research Institute (CSIR), Lucknow, Uttar Pradesh 226031, India

ARTICLE INFO

Keywords:
Oncostatin M
M2 polarization
Hypoxia
mTORC2
Akt
Metastasis

ABSTRACT

Oncostatin M (OSM), an inflammatory cytokine belonging to the interleukin-6 (IL-6) superfamily, plays a vital role in multitude of physiological and pathological processes. Its role in breast tumor progression and metastasis to distant organs is well documented. Recent reports implicate OSM in macrophage M2 polarization, a key pro-tumoral phenomenon. M2 polarization of macrophages is believed to promote tumor progression by potentiating metastasis and angiogenesis. In the current study, we delineated the mechanism underlying OSM induced macrophage M2 polarization. The findings revealed that OSM skews macrophages towards an M2 polarized phenotype via mTOR signaling complex 2 (mTORC2). mTORC2 relays signals through two effector kinases i.e. PKC-α and Akt. Our results indicated that mTORC2 mediated M2 polarization of macrophages is not dependent on PKC-α and is primarily affected via Akt, particularly Akt1. *In vivo* studies conducted on 4T1/BALB/c mouse orthotropic model of breast cancer further corroborated these observations wherein *i.v.* reintroduction of mTORC2 abrogated monocytes into orthotropic mouse model resulted in diminished acquisition of M2 specific attributes by tumor associated macrophages. Metastasis to distant organs like lung, liver and bone was reduced as evident by decrease in formation of focal metastatic lesions in mTORC2 abrogated monocytes mice. Our study pinpoints key role of mTORC2-Akt1 axis in OSM induced macrophage polarization and suggests for possible usage of Oncostatin-M blockade and/or selective mTORC2 inhibition as a potential anti-cancer strategy particularly with reference to metastasis of breast cancer to distant organs such as lung, liver and bone.

1. Introduction

The solid tumors are not isolated niche of transformed cancer cells alone; they also include a complex and heterologous peritumoral stroma comprised of non cancer cells such as fibroblasts, smooth muscle cells, neutrophils and macrophages [1]. Of particular significance are macrophages, as they represent the most abundant subpopulation of immune cells infiltrating into tumor stroma and constitute 5–40% of tumor mass [2]. While cytotoxicity of macrophages in the early immune response contributes to tumor killing, at later stages i.e in malignant tumors, macrophages promote tumor progression resulting in poor patient prognosis [3]. These diametrically opposite functions are possible due to tremendous degree of heterogeneity and plasticity which is a hallmark of monocyte-macrophage lineage cells [4]. Dictated by cytokine milieu of the tumor microenvironment, macrophages rapidly undergo phenotype switching to acquire either of the two functionally distinct extremes of physiological/phenotypic continuum viz. classically activated M1 polarized state or alternatively activated M2 polarized state [5,6]. The M1 macrophages predominantly secrete pro-inflamatory mediators to trigger inflammatory responses and are

Abbreviations: OSM, Oncostatin M; mTORC2, mammalian target of Rapamycin complex 2; Nx-Ca-CM, normoxic cancer cell conditioned media; Hx-Ca-CM, hypoxic cancer cell conditioned media; Arg-1, arginase-1; COX-2, cyclooxygenase-2; PtdIns(3,4,5)P_3, phosphotidyl inositol (3,4,5)-trisphosphate

* Corresponding author at: Division of Toxicology and Experimental Medicine, Central Drug Research Institute, Lucknow, India.
E-mail address: smriti_bhadauria@cdri.res.in (S. Bhadauria).

https://doi.org/10.1016/j.cyto.2018.03.032
Received 20 August 2017; Received in revised form 19 March 2018; Accepted 21 March 2018
Available online 03 April 2018
1043-4666/

tumoricidal. In contrast, the M2 macrophages mainly produce anti-inflammatory mediators for dampening the inflammatory responses and exhibit pro-tumoral functions [7]. Although, both the subtypes have been observed in tumor, the majority of tumor associated macrophages (TAMs) exhibit M2 specific attributes [1]. Mounting evidence suggests that the infiltrated macrophages initially have an immature or anti-tumoral M1-polarized phenotype; however continued presence in tumor microenvironment polarizes them to pro-tumoral M2-skewed TAMs [8]. Better discernment of mechanisms governing macrophage M2 polarization particularly in consideration of unique physiochemical features of tumor microenvironment is well warranted as this is likely to unravel key molecular determinants which in turn could be targeted for attenuating macrophage M2-polarization and/or their reprogramming to M1 subtype. It is proposed that by way of depriving tumor cells of important growth support derived from M2 macrophages, and/or enhancing the anti-tumor immune response contributed by M1 macrophages, this could serve as effective anti-cancer strategy [1].

Hypoxic tumor milieu has been postulated as one of the most probable causes of macrophage M2-polarization [8]. Consistent with this, the hypoxic area of human endometrial [9], breast [10,11], prostate [12] and ovarian carcinomas [13] are known to have large congregation of M2 like TAMs. Although the evidence in support of hypoxic microenvironment being instrumental in macrophage recruitment and polarization are gradually mounting [8], the exact mechanism underlying sequestration of macrophages to hypoxic regions and their subsequent polarization is poorly understood and warrants an in-depth investigation. We recently demonstrated Oncostatin M (OSM) as one of the key mediators for recruitment and polarization of macrophages with in hypoxic cancer milieu though the underlying mechanism of OSM induced Macrophage M2 polarization remains obscure [14].

OSM, a member of IL-6 family of cytokine is produced by inflammatory cells as well as by some tumor cells and primary human cells eg. oesteoblasts [15,16]. Ample experimental evidence suggest for a key role of OSM during tumor progression particularly breast cancer [17]. While normal mammary epithelial cells express lower levels of OSM, its levels are markedly upregulated in ductal carcinoma *in situ* and invasive breast carcinoma [18]. In addition, other tumor microenvironment subpopulations such as tumor-associated macrophages and neutrophils also express and release high levels of OSM in response to breast cancer cells [19]. The essential prerequisites for metastatic transformation of cancer cells viz. epithelial to mesenchymal transition [20], cell-substrate detachment and ECM degradation [17,21], all are positively modulated by OSM, thus pointing towards OSM as one of the key actuators of cancer metastasis. Accordingly, targeting OSM resulted in diminished mammary tumor metastasis and osteolytic bone degradation thereby designating OSM as a liable therapeutic target for impeding bone metastasis and bone erosion in breast cancer patients [22]. OSM like other IL-6 family cytokines like LIF promotes macrophage M2 polarization in ovarian cancer model [23]. While the mechanisms by which OSM promotes tumor cell intrinsic pathways of cancer progression are well documented [24], however the mechanism underlying M2 polarization remains obscure. Thus in current study, we set out to identify the mechanism by which OSM may educate macrophages to acquire the pro-tumoral M2 polarized phenotype. Particular emphasis was laid on hypoxic tumor environment as hypoxia is known to selectively promote macrophage M2-polarization via hypoxic cancer cell derived OSM.

2. Materials and methods

2.1. Cell culture

Human leukemia monocyte THP-1 cells, human mammary cancer-derived cells (MCF-7, MDA-MB-231) were procured from ATCC. Cells were maintained in RPMI 1640 or DMEM, respectively, using standard mammalian cell culture methods. THP-1 cells were differentiated to macrophages using 30 nM Phorbol 12-myristate 13-acetate (PMA) according to Daigneault et al [25]. Human PBMCs were allowed to differentiate into resting macrophages after 7 days of culture in RPM1 1640. Non-adherent cells were removed by discarding the media and washing with PBS. Differentiation was ascertained by evaluating the expression of macrophage specific markers viz, CD16 and Myeloid Cell Leukemia sequence-1(Mcl-1).

2.2. Hypoxia treatment

Cancer cells were exposed to hypoxia using hypoxia chamber (Stem cell technologies, USA) maintained at low oxygen levels (1% O_2, 5% CO_2 and 94% N_2). The culture were placed in the hypoxia chamber and existing culture medium was replaced with deoxygenated RPMI 1640/DMEM. Deoxygenated medium was prepared before each experiment by equilibrating the medium with a hypoxic gas mixture containing 1% O_2, 5% CO_2 and 94% N_2 at 37 °C. The oxygen concentration in the hypoxic chamber and the exposure medium was monitored by using an oxygen indicator (Forma Scientific Marietta, OH).

2.3. Fluorescence immunocytochemistry and flow cytometry

For fluorescence immunocytochemical detection of M2-polarized macrophage, the culture supernatant of control and experimental macrophage cultures (grown in sterile coverslips) was removed and cells were washed twice with DPBS, followed by fixation with 3.7% paraformaldehyde at 37 °C. After washing with DPBS thrice the specimen were blocked with 5% BSA for 1 h. Thereafter cells were incubated overnight with anti-human CD206 or anti-human CD163 mouse antibodies (1:100) at 4 °C. Specimens were then incubated with Alexa fluor 555 conjugated anti-mice IgG (1:200) for 1 h. Finally cells were mounted in prolong gold antifade-DAPI aqueous mounting media and visualized (200X) using Carl Zeiss florescence microscope. For flowcytometry based detection of CD206 positive M2-macrophges, the control and experimental macrophage cultures were fixed with 3.7% paraformaldehyde for 20 min at 37 °C washed with PBS twice and harvested for flowcytometry. Cells were suspended in PBS and incubated with FITC conjugated anti-CD206 antibody for 1 h at 4 °C. Finally, 10,000 viable cells were analyzed by flowcytometry using FACS Calibur flowcytometer (BD Biosciences, USA).

2.4. Immunoblotting

Total protein were extracted from cells using radio immunoprecipitation assay (RIPA) buffer containing protease and phosphatase inhibitors. Protein content in the supernatants was determined using Lowry's Folin method [26] and separated on 6 and 12% SDS-PAGE. Blots were incubated with corresponding primary and HRP-conjugated secondary antibodies. Peroxidase activity was analyzed with the ECL chemiluminescence substrate system (USA).

2.5. Real-time PCR

Total RNA was isolated with Trizol reagent (Molecular Research Center), and cDNA was obtained from 2 μg of total RNA using High Capacity cDNA Reverse Transcription Kit. Quantitative PCR was performed on a Light Cycler 480 System (Roche) in 96-well plates using SYBR Green qPCR Master Mix in accordance with manufacturer's protocol. Data were analyzed using the Roche Light Cycler 480 software (Version 1.5). Cp and Ct were calculated by the Second Derivate Maximum Method. The amount of the target mRNA was examined and normalized to the β-actin gene mRNA. The relative expression ratio of a target gene was calculated as described by Pfaffi [27]. Results represent data from three separate experiments. Forward and Reverse Primer sequence is given in suppl.8

2.6. Short interfering RNA (siRNA) transfection

Briefly, 4×10^5 cells were differentiated in RPMI supplemented with 10% CSFBS and were transfected with 600 pM of pooled pre-validated siRNAs using siPort NeoFX reagent (Ambion, USA). 24 h after transfection, the culture media was replaced with fresh media. Cells were further maintained for 24 h and subsequently harvested for respective experiments. The sources of siRNAs has been mentioned in suppl. 13.

2.7. Plasmids and transfection

All plasmid transfection experiments were carried out using pre-validated and quantified plasmids using Lipofectamine LTX (3000) reagent according to manufacturer's instruction. The sources of Plasmids has been mentioned in suppl. 13.

2.8. Animals

All procedures with mice were done under an Institutional Animal Care and Use Committee-approved protocol (#IAEC/2014/141). Female BALB/c mice of 4 weeks age were procured from institutional laboratory animal facility. Mice were housed in polypropylene cages in a group of five /cage. They were maintained on pellet diet, water *ad libitum,* and regular alternate cycles of 12 h light and darkness. Prior to tumor initiation, animals were acclimatized for 7 days.

2.9. Subcutaneous orthotropic mammary tumor model of 4T1 cells in BALB/c mice

4T1/BALB/c tumors were initiated by injecting 1×10^6 viable 4T1 cells subcutaneously in the T4 of mammary fat pad of the BALB/c mice. After two days the animals were boosted by injecting another dose of 1×10^6 viable 4T1 cells at the initial injection site. The growth of tumor was monitored throughout the experiment with tumor size being measured daily using vernier calipers and represented in terms of tumor volume [$= 4/3\pi$ X(Long axis/2) X(Short axis/2)]. After the tumor attained a size of 8–10 mm^3, the tumor bearing mice were randomized into 4 groups based on tumor volume with each group comprising of 4 mice/group. Mouse PBMCs were isolated using Ficoll Plaque density gradient 1.084. The mice were treated with GdCl3 10 mg/kg once a week through caudal vein. The isolated monocytes were cultured in RPMI media supplemented with 10% FBS and 1% antimycotic and antibiotic. Mouse monocytes were transfected with the siRNA targeted against Rictor and Quantum-dots (Q-Dots) before being reintroduced to the mice [28]. Q-dots also known as quantam dots are labeled nanocrystals which permeate in the cells owing to their small sizes in nanometer range. Once inside the cells they grow in sizes due to which they get entrapped as they cannot diffuse out of cell. They give out red fluorescence and expressed by them till 7 generations. 2 weeks later all the mice were killed by cervical dislocation. The tumor was removed and stored for further examination. Liver, lung and bone were excised. The animal groups are as described in suppl. 12.

2.10. Isolation of macrophages from tumor

Tumor tissue was cut into 2 mm fragments, followed by collagenase digestion (0.3 mg/ml). The suspension was filtered through a 70 μm stainless steel wire mesh to generate single cells which were then processed for flowcytometric detection, immunoflurocsence microscopy of CD206 and RT-PCR for mRNA expression of Arginase-1 and Cycloxygenase-2.

2.11. H&E staining

H&E staining was performed on formalin-fixed, paraffin embedded tissue sections (5 μm). Tissue architecture and metastatic foci were visualized by examining hematoxylin and eosin stained section of each specimen (200×) using Leica11521249BZ:00 DFC450C bright field/fluorescence microscope.

2.12. MicroCT analysis

A high-resolution X-ray micro-computed tomographic (μCT) for two-dimensional (2D) and three-dimensional (3D) assessment of bones (excised bones) were carried out using a Sky Scan 1076 μCT scanner (SkyScan, Ltd, Kartuizersweg, Kontich, Belgium). Briefly, after scanning bone samples at a nominal resolution (pixels) of 9 μm and X-ray source of 50 kV-201 μA, cross-sectional reconstruction was made using SkyScan Nrecon software based on a modified Feldkamp algorithm. To analyze trabecular region and create 2D trabecular network model, region of interest (ROI) was drawn on a total of 100 slices in the region of secondary spongiosa (SS) situated 1.5 mm away from the distal border of growth plate (GP) excluding primary spongiosa (PS) and cortical bone. For whole bone lesion model ROI was drawn on a total 500 slices including both trabecular and cortical region of tibia. Bone model was created by using CTAn and CTVol software.

2.13. Statistical analysis

Data were summarized as Mean and SEM. Groups were compared by one-way analysis of variance (ANOVA) followed by Newman–Keuls post hoc test. A two-tailed $p < 0.05$ was considered statistically significant.

3. Results

3.1. Hypoxic cancer cell secretome induced M2-polarization of macrophages was associated with potentiated mTOR signaling complex-2

Hypoxic cancer cell secretome skews macrophages towards an M2-polarized phenotype [14]. Akt isoforms (differentially regulate) play a central role in macrophage polarization [29]. Because mTORC2 is essential for full activation of Akt, we sought to assess mTORC2 activation status during hypoxic cancer secretome induced macrophage M2-polarization. In addition to enhanced presence of M2 specific attributes, the level of key mTORC2 activation marker viz. p-Ser^{2481}-mTOR was markedly upregulated in macrophages (THP-1 and HuPBMMCs drived macrophages) incubated (for 24 h) with CM harvested from breast cancer cells subjected to varying durations (3, 6 and 24 h) of hypoxia (Fig. 1A and suppl.2A, 3A). Similar to M2-polarization, the extent of mTORC2 potentiation was proportional to the duration of hypoxia (Fig. 1B and Suppl.2B, 3B). Phosphorylation status of both PI3K dependent (Akt) and independent (PKC-α) downstream targets of mTORC2 was assessed as an additional confirmatory measure of mTORC2 activation. Increased HM phosphorylation of key downstream targets viz p-Ser^{473}Akt and p-Ser^{657}PKCα further corroborate heightened mTORC2 activation in macrophages by hypoxic cancer cell secretome. The level of M2 specific CD206 expression levels and p-Ser^{2481}-mTOR exhibited maximal elevation in macrophages that were incubated with CM harvested from 6hrs hypoxic cells with no further increase when incubated with 24 h hypoxic cells. Therefore, to develop the data further, we next incubated macrophages for varying durations (0, 12, 24 h) with CM harvested from breast cancer cells MDA-MB-231 subjected to hypoxia (Hx-Ca-CM) for a fixed duration (6 h) and evaluated mTORC2 activation status. Macrophages exhibited a characteristic duration dependent increase in the activation status of mTORC2 as reveled by elevated p-Ser^{2481}-mTOR, p-Ser^{473}Akt and p-Ser^{657}PKCα levels in concurrent to upregulation in markers of M2 polarization (Fig. 1C and D). To ascertain that breast cancer cells experienced hypoxia, HIF-1α expression was evaluated in MDA-MB-231 and MCF-7 (suppl.1)

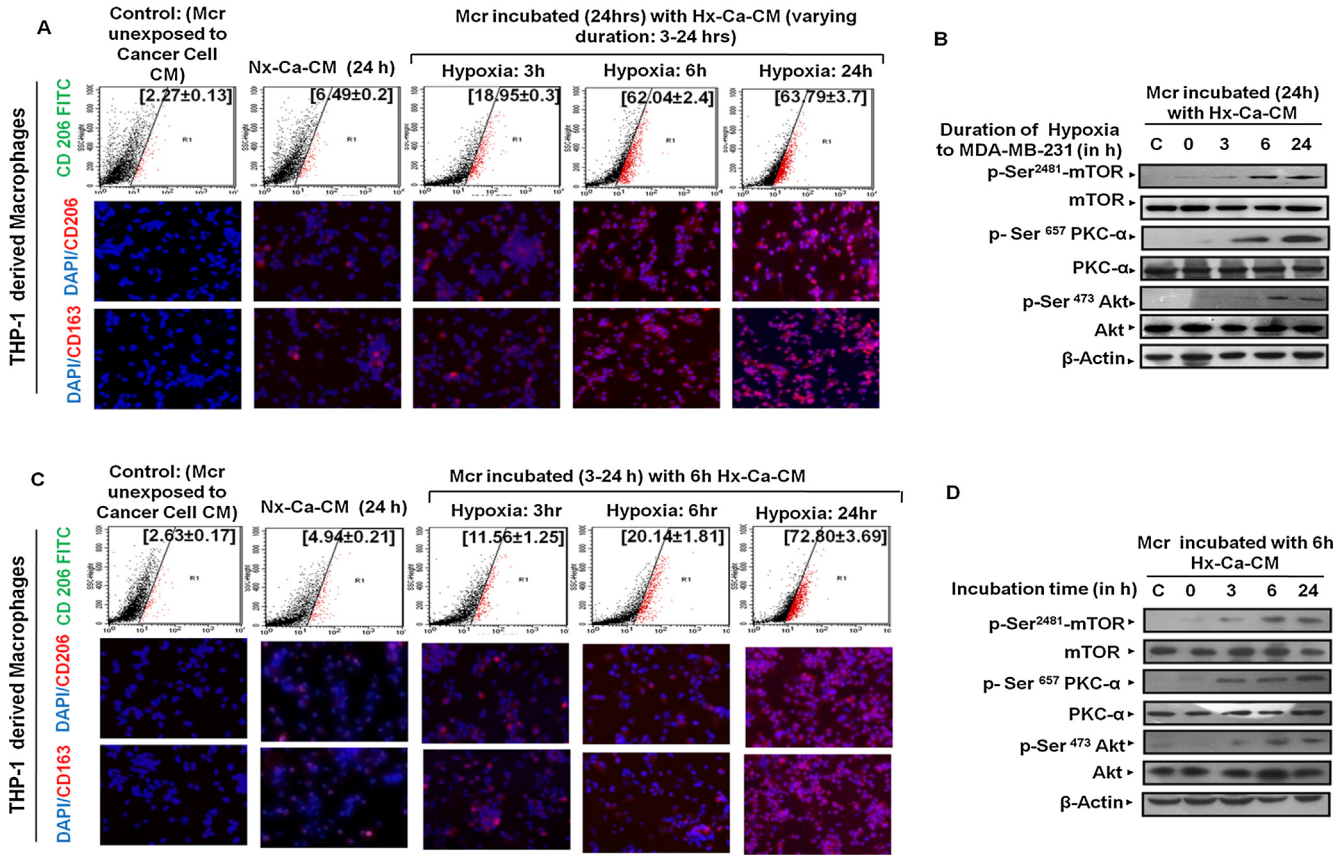

Fig. 1. Hypoxic cancer cell secretome induced M2-polarization of macrophages was associated with potentiated mTOR signaling complex-2. (A) THP-1 derived macrophages were incubated with conditioned media (CM) from hypoxia primed (3, 6 and 24 h) breast cancer MDA-MB-231 cells (Hx-Ca-CM) for 24 h as indicated in the figure, followed by phenotypic evaluation using flowcytometry and immunocytochemistry. Representative flowcytometry data and photomicrographs depicting M2 polarization of THP-1 derived macrophages using M2 surface markers anti-CD206 and anti-CD163. (B) Lysates of THP-1 derived macrophages incubated with conditioned media (CM) from hypoxia primed (3, 6 and 24 h) breast cancer MDA-MB-231 cells (Hx-Ca-CM) for 24 h as indicated in figure were resolved through SDS-PAGE and western blots of the membranes were detected using antibodies against p-Ser^{2481}mTOR, mTOR, p-Ser^{657}PKC-α PKC-α, p-Ser^{473}Akt, Akt and β-actin. (C) THP-1 derived macrophages were incubated with conditioned media (CM) from Hypoxia primed (6 h) breast cancer MDA-MB-231 cells (Hx-Ca-CM) for (3, 6 and 24 h) as indicated in figure, followed by phenotypic evaluation using flowcytometry and immunocytochemistry. Representative flowcytometry data and photomicrographs depicting M2 polarization of THP-1 derived macrophages using M2 surface markers anti-CD206 and anti-CD163. (D) Lysates of THP-1 derived macrophages incubated with conditioned media (CM) from Hypoxia primed (6 h) breast cancer MDA-MB-231 cells (Hx-Ca-CM) for (3, 6 and 24 h) as indicated in figure were resolved through SDS-PAGE and western blots of the membranes were detected using antibodies against p-Ser^{2481}mTOR, mTOR, p-Ser^{657}PKC-α, PKC-α, p-Ser^{473}Akt, Akt and β-actin.

3.2. Rictor directed modulation of mTORC2 activity resulted in altered M2-polarization of THP-1 derived macrophages by hypoxic cancer cell secretome

Precisely concurrent activation of mTORC2 signaling during Hx-Ca-CM induced M2 polarization suggested that mTORC2 pathway could be coordinating the process. To examine this hypothesis, we first evaluated the effect of mTORC2 abrogation on macrophage M2 polarization. The mTORC2 signaling was obstructed in macrophages via siRNA mediated downregulation of Rictor, a key regulatory/structural subunit essential for functionally intact mTORC2 [30]. Compared to normal macrophage cultures, the ones incubated with cancer cell CM (Ca-CM) exhibited M2-polarized macrophages to a greater extent as revealed by flowcytomety based detection of M2-specific cell surface marker viz. CD206 and q-RT-PCR based mRNA expression level analysis of M2-specific functional markers viz Arginase-1 (Arg-1) and Cyclooxygenase-2 (COX-2). As expected, compared to Nx-Ca-CM, exposition of macrophages to Hx-Ca-CM resulted in elevated CD206 + ve cell count, however the macrophages cultures where mTORC2 signaling was obstructed prior to exposition to normoxic or hypoxic conditioned media, the CD206 positive cell count was much diminished as compared to corresponding control cells. The mRNA expression levels of M2-specific functional markers viz. Arg-1 and COX-2 exhibited similar trend (Fig. 2A and Suppl.5). The data indicated that impaired mTORC2 signaling not only results in diminished M2 polarization of macrophages by Hx-Ca-CM particularly, but even the basal level of macrophage phenotype switching following their incubation with Nx-Ca-CM gets markedly hampered. The role of mTORC2 was further ascertained by augmenting the mTORC2 signaling in macrophages via ectopic over expression of Rictor. Results revealed that compared to control macrophages, the ones with heightened mTORC2 signaling exhibited increased presence of M2-specific attributes. Amongst the macrophages exposed to Nx-Ca-CM, the Rictor overexpression mediated increased mTORC2 signaling was sufficient to produce robust increase in M2-polarization as revealed by increased CD206 + ve cell count, Arg-1 and COX-2 mRNA expression levels. Rictor overexpression also culminated in enhanced Hx-Ca-CM induced M2-polarization albeit to a lesser degree as compared to corresponding macrophages (Rictor over expressing) exposed to Nx-Ca-CM. The results indicated for regulatory role of mTORC2 during M2-polarization of macrophages particularly in response to their exposure to hypoxic cancer cell secretome (Fig. 2B).

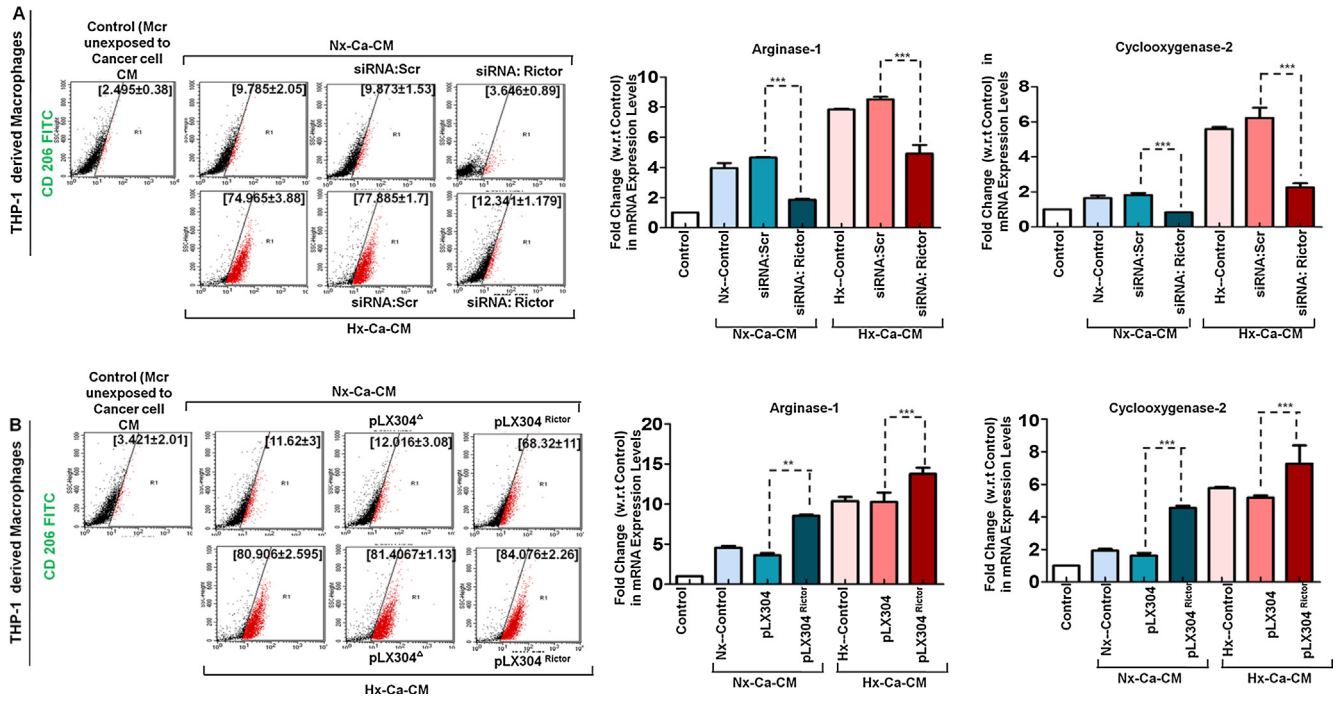

Fig. 2. Rictor directed modulation of mTORC2 activity resulted in altered M2-polarization of THP-1 derived macrophages by hypoxic cancer cell secretome. (A) THP-1 derived macrophages transfected with Scrambled (control) siRNA or siRNA directed against rictor were primed with Nx-Ca-CM and Hx-Ca-CM as indicated in figure. Representative flowcytometry and RT-PCR analysis of M2 specific surface (CD206) and functional markers (Arg-1 and COX-2). (B) THP-1 derived macrophages transfected with control vector (PLX304) or PLX304-Rictor were primed with Nx-Ca-CM and Hx-Ca-CM as indicated in figure. Representative flowcytometry and RT-PCR analysis of M2 specific surface (CD206) and functional markers (Arg-1 and COX-2). RT-PCR experiment was done in duplicates thrice. Bars represent relative fold change in expression ± SEM. $^{*}P < 0.05$, $^{**}P < 0.01$ and $^{***}P < 0.001$.

3.3. Macrophages exposed to hypoxic cancer cell CM, exhibited potentiated mTORC2 in an Oncostatin M (OSM) dependent manner

Because OSM is an important constituent of hypoxic cancer cell secretome and a key mediator of macrophage M2-polarization, we next studied if OSM could be involved in activation of mTORC2 pathway in the macrophages following their exposition to hypoxic cancer cell secretome. Compared to macrophages incubated with Nx-Ca-CM, the ones incubated with Hx-Ca-CM exhibited potentiated mTORC2 signaling as revealed by upregulated p-Ser^{2481}-mTOR, p-Ser^{473}Akt and p-Ser^{657}PKCα levels. The neutralizing antibody mediated functional blockade of OSM attenuated the mTORC2 activation caused by both Hx-Ca-CM and OSM supplemented Nx-Ca-CM. Furthermore, compared to macrophages exposed to Nx-Ca-CM, the ones exposed to recombinant OSM (0.2 μg/ml) supplemented Nx-Ca-CM exhibited potentiated mTORC2 pathway (Fig. 3A and suppl.6A). Results indicated that activation of mTORC2 during macrophage M2 polarization was dependent on OSM. The characteristic concentration dependent potentiation of mTORC2 in THP-1 derived macrophages following treatment with Nx-Ca-CM supplemented with varying concentration OSM further underlined the involvement of OSM (Fig. 3B).

3.4. OSM induced macrophage M2 polarization is mediated by mTORC2

As the Hx-Ca-CM induced M2 polarization was mediated by mTORC2 activation, we set out to ascertain if mTORC2 is involved in OSM induced M2 macrophage polarization. To this end, we obstructed mTORC2 signaling in macrophages using siRNA against rictor. Results indicated increased expression of M2 macrophage surface marker CD206 and CD163 in macrophages treated with OSM compared to macrophages exposed to Nx-Ca-CM. Similarly, the mRNA expression of M2 functional marker Arg-1 and COX-2 were also upregulated in OSM treated macrophages. This effect of OSM was reverted in macrophages where mTORC2 was obstructed before OSM treatment. Thus intact mTORC2 activity is essential for M2 macrophage polarization mediated by OSM as even the basal level of M2 polarization was inhibited due to silencing of rictor in macrophages. To confirm the mTORC2 activity mediating M2 polarization Rictor was overexpressed ectopically in macrophages. Results indicated that macrophages with heightened mTORC2 activity displayed enhanced expression of M2 macrophages surface markers CD206 and CD163 in addition to functional markers Arg-1 and COX-2 compared to macrophages transfected with backbone vector. The rictor overexpressed macrophages treated with OSM expressed enhanced M2 characteristics compared to vector transfected macrophages treated with OSM. Thus it is evident that mTORC2 is indispensible to M2 macrophage polarization caused by OSM. IL-4 is a well known classical mediator of M2 polarization. Hence, we evaluated whether IL-4 induced M2 polarization is also mediated by activation of mTORC2 pathway in the macrophages. Compared to macrophages incubated in normal unconditioned media the ones incubated with IL-4 exhibited potentiated mTORC2 activation, evident by upregulation of p-Ser^{2481}-mTOR, and its effectors p-Ser^{473}Akt and p-Ser^{657}PKCα levels (Suppl.7A). These observations indicated that IL-4 induced M2 polarization is circumstantial to mTORC2 activation. Modulation of mTORC2 via silencing and overexpression of rictor revealed that mTORC2 mediates IL-4 induced M2 polarization (suppl.7B).

3.5. Hypoxic cancer cell CM induced macrophage M2 polarization via OSM is affected by mTORC2 through Akt and not PKCα

Akt and PKCα are two key downstream effectors through which mTORC2 relays the signals. Having established key role of mTORC2 in OSM induced macrophage M2-polarization, we next decided to elucidate as to which of the two key downstream cascades is primarily employed by mTORC2 for affecting OSM induced macrophage M2-polarization. To this end, prior to OSM treatment THP-1 derived

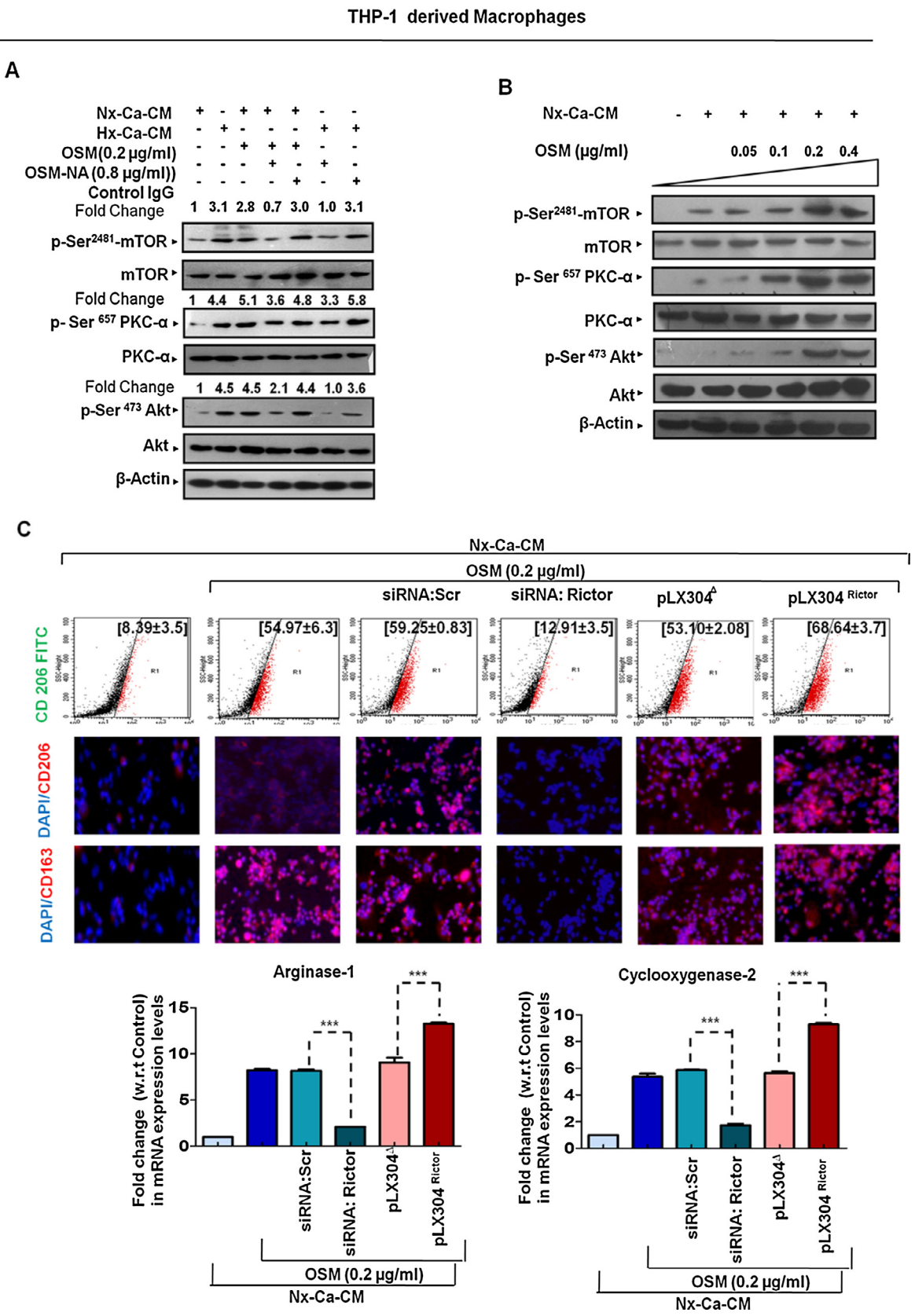

(caption on next page)

macrophages were treated with either staurosporine (100 nM), potent inhibitor of PKC-α at stipulated concentration was found to inhibit PKC-α [31,32] or Akt inhibitor IV, a cell permeable and reversible benzimidazole compound that inhibits Akt phosphorylation/activation by targeting the ATP binding site of a kinase upstream of Akt, but downstream of PI3K [33]. Staurosporine treatment did not impede OSM

Fig. 3. Macrophages exposed to hypoxic cancer cell CM, exhibited potentiated mTORC2 in an Oncostatin M (OSM) dependent manner and OSM induced macrophage M2 polarization is mediated by mTORC2. (A) THP-1 derived macrophages incubated with Nx-Ca-CM, Hx-Ca-CM, Oncostatin M (OSM 0.2 μg/ml), neutralizing antibody against OSM (OSM NA 0.8 μg/ml) and IgG as indicated in the figure. Macrophages incubated with IgG served as isotype control (lane 5 and lane 7). Lysate of the cells were resolved through SDS-PAGE and western blots of the membranes were detected using antibodies against p-Ser^{2481}mTOR, mTOR, p-Ser^{657}PKC-α PKC-α, p-Ser^{473}Akt, Akt and β-actin. (B) THP-1 derived macrophages incubated with Nx-Ca-CM and exposed to different concentrations of OSM i.e. 0.05, 0.1, 0.2, 0.4 μg/ml. Lysate of the cells were resolved through SDS-PAGE and western blots of the membranes were detected using antibodies against p-Ser^{2481}mTOR, mTOR, p-Ser^{657}PKC-α PKC-α, p-Ser^{473}Akt, Akt and β-actin. (C) THP-1 derived macrophages transfected with Scrambled (control) siRNA or siRNA directed against rictor, control vector (PLX304) or PLX304-Rictor were primed with Nx-Ca-CM and treated with OSM (0.2 μg/ml) as indicated in figure. Representative flowcytometry data and photomicrographs depicting M2 polarization using M2 surface markers anti-CD206 and anti-CD163 and RT-PCR analysis of M2 specific functional markers (Arg-1 andCOX-2). All experiments were performed thrice and integrated density in western blots was determined by densitometry analysis using thermo my image analysis software. Results show relative levels of p-Ser^{2481}mTOR, p-Ser^{657}PKC-α -α, p-Ser^{473}Akt, i.e. ratio between integrated density of p-Ser^{2481}mTOR/ mTOR, p-Ser^{657}PKC-α/PKC-α, and p-Ser^{473}Akt/Akt. RT-PCR experiment was done in duplicates thrice. Bars represent relative fold change in expression ± SEM. $^{*}P < 0.05$, $^{**}P < 0.01$ and $^{***}P < 0.001$.

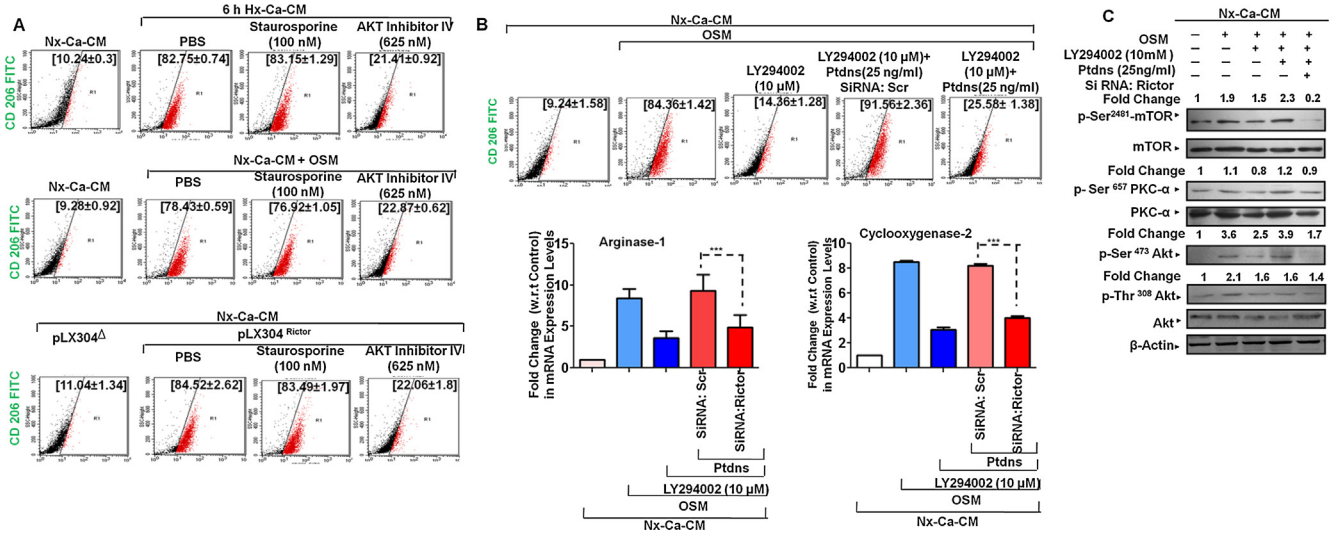

Fig. 4. Hypoxic cancer cell CM induced macrophage M2 polarization via OSM is affected by mTOR through Akt and not PKC-α. (A) THP-1 derived macrophages were pretreated with staurosporin 100 nM (PKCα inhibitor) or Akt kinase inhibitor (625 nM) and incubated with Hx-Ca-CM or OSM (0.2 μg/ml) or transfected with PLX304-Rictor as indicated in figure. Representative flowcytometry data depicting M2 polarization using M2 surface markers anti-CD206. (B) Scrambled siRNA or siRNA directed against rictor transfected THP-1 derived macrophages pretreated with LY294002 and stimulated with OSM (0.2 μg/ml) or (PtdIns(3,4,5)P_3) as indicated in the figure. Representative flowcytometry and RT-PCR analysis of M2 specific surface (CD206) and functional markers (Arg-1 and COX-2). (C) Scrambled siRNA or siRNA rictor transfected THP-1 derived macrophages were pretreated with LY294002 and stimulated with OSM (0.2 μg/ml) or (PtdIns(3,4,5)P_3) as indicated in the figure. Lysates of above cells were resolved through SDS-PAGE and western blots of the membranes were detected using antibodies against p-Ser^{2481}mTOR, mTOR, p-Ser^{657}PKC-α PKC-α, p-Ser^{473}Akt, p-Thr^{308}Akt, Akt and β-actin. All experiments were performed thrice and integrated density in western blots was determined by densitometry analysis using thermo my image analysis software. Results show relative levels of p-Ser^{2481}mTOR, p-Ser^{657}PKC-α -α, p-Ser^{473}Akt, p-Thr^{308}Akt, i.e. ratio between integrated density of p-Ser^{2481}mTOR/mTOR, p-Ser^{657}PKC-α/PKC-α, p-Ser^{473}Akt/Akt and p-Thr^{308}Akt/Akt. RT-PCR experiment was done in duplicates thrice. Bars represent relative fold change in expression ± SEM. $^{*}P < 0.05$, $^{**}P < 0.01$ and $^{***}P < 0.001$.

or hypoxic cancer cell CM induced M2-polarization of THP-1 macrophages. On the other hand, OSM or hypoxic cancer cell CM induced M2-polarization of THP-1 macrophages was markedly impeded in presence of Akt inhibitor IV. Results indicated that Akt but not PKC α was indispensable for mTORC2 to affect OSM induced M2 polarization (Fig. 4A). We validated the inhibition of PKC-α via PKC-α dependent phosphorylation of p65NF-kB at ser276. This phosphorylation was inhibited by staurosporin. Results are incorporated in suppl.8.

PI3K is one of the key upstream positive modulator of Akt activity. There is ample evidence for role of PI3K in macrophage M2 polarization. Interestingly, OSM is known to potentiate PI3K signaling. Furthermore, while mTORC2 is not a direct downstream target for PI3K, there are ample evidence for existence of crosstalk between mTORC2 and PI3K signaling. Thus, OSM induced M2 polarization could at least in part be a consequence of PI3K/Akt activation rather than that of mTORC2 *per se.* Therefore, we set out to study role PI3K/Akt during OSM induced M2 polarization with respect to essentiality of mTORC2. PI3K generates specific phosphatidyl inositol triphosphate (PIP_3) which in turn are recognized by phosphoinositide-dependent kinases (PDKs). One specific PDK i.e PDK1 phophorylates Akt at Ser308 resulting in its activation. While full activation of Akt requires its subsequent phosphorylation at Ser473 at its hydrophobic motif (HM) primarily by an activated mTORC2, but several studies reveal that PI3K activation is sufficient to restore Akt Ser473 phosphorylation and activation in cells lacking mTORC2. Interestingly, mTORC2 is directly activated by (PtdIns(3,4,5)P_3) [34]. Surprisingly, pretreatment (2 h) with PI3K inhibitor, LY294002 completely reversed OSM induced macrophage M2 polarization. This result pointed towards possibility that M2 polarization by OSM was in actuation attributable to PI3K /Akt pathway, while mTORC2 activation in presence of OSM could only be a subsidiary event (owing to (PtdIns(3,4,5)P_3) buildup), completely dissociated with M2-polarization. To rule out this possibility additional experiments were carried out using exogenously supplied (PtdIns(3,4,5)P_3) in presence of PI3K inhibitor LY294002. While addition of (PtdIns(3,4,5)P_3) restored OSM induced M2 polarization even in presence of LY29400, when macrophages having abrogated mTORC2 (via siRNA mediated silencing of rictor) were subjected to similar treatment (OSM + LY29400 + (PtdIns(3,4,5)P_3) the M2 polarization remained much impeded as compared to macrophages treated with OSM alone (Fig. 4B and suppl.9). Results indicated that even if Akt is active, abrogation of mTORC2 will markedly impede OSM induced macrophage polarization. Our results indicated for indispensability of mTORC2 for

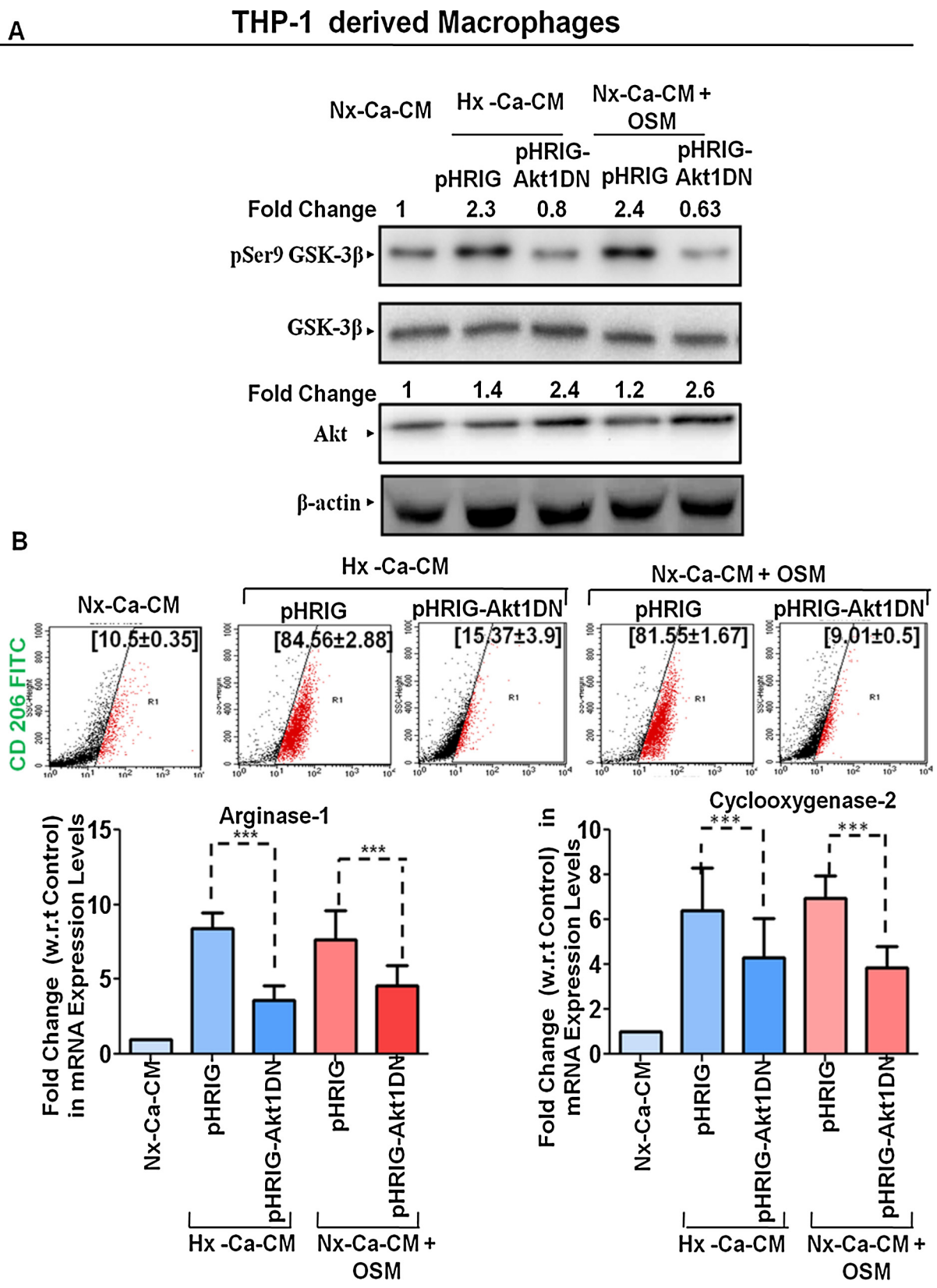

Fig. 5. Distinct Role of Akt1 during OSM induced Macrophage M2 Polarization. (A) THP-1 derived macrophages were transfected with control pHRIG vector or Akt dominant negative gene construct (pHRIG-Akt1DN) and treated with either Hx-Ca-CM or OSM (0.2 μg/ml) as indicated in the figure. Lysates of above cells were resolved through SDS-PAGE and western blots of the membranes were detected using antibodies against p-ser^{9}GSK3-β, GSK3-β, Akt and β-actin. (B) THP-1 derived macrophages transfected with Control pHRIG vector or Akt dominant negative gene construct (pHRIG-Akt1DN) and were treated with either Hx-Ca-CM or OSM (0.2 μg/ml) as indicated in the figure. Representative flowcytometry data depicting M2 polarization using M2 surface markers anti-CD206 and RT-PCR analysis of M2 specific functional markers (Arg-1 and COX-2). All experiments were performed thrice and integrated density in western blots was determined by densitometry analysis using thermo my image analysis software. Results show relative levels p-Ser^{9}GSK3-β and Akt i.e. ratio between integrated density of p-Ser^{9}GSK3-β/ GSK3-β and Akt/ β-actin. RT-PCR experiment was done in duplicates thrice. Bars represent relative fold change in expression ± SEM. $^{*}P < 0.05$, $^{**}P < 0.01$ and

OSM induced macrophage polarization. To ascertain PI3K inhibition, western blotting was performed to evaluate the levels of p-Thr^{308}Akt (Fig. 4C).

Arranz et al. (2012) showed that inhibition of Akt1 give rise to M1 macrophages whereas inhibition of Akt2 give rise to M2 macrophages [29]. To further corroborate this study in our system, THP-1 derived and HuPBMCs derived macrophages were transfected Akt dominant negative gene construct (pHRIG-Akt1DN). To ascertain successful transfection western blotting was performed. There was decrease in phosphorylation of GSK3-β at Ser9 which is target of Akt (Fig. 5A and suppl.10). The major finding in this set of experiment was effect of pHRIG-Akt1DN on M2 polarization of macrophages. Results revealed that ablation of Akt1 completely abrogated OSM induced macrophage M2 polarization thereby establishing this particular isoform as a key effector for OSM induced mTORC2 mediated macrophage M2-polarization (Fig. 5B and suppl.10B).

3.6. In vivo myeloid specific rictor abrogation resulting in regression of 4T1 primary tumor and concurrently diminished recruitment and M2 polarization of tumor associated macrophages and impeded distant tissue metastasis to liver, lung and bone

To further substantiate the above findings, the results were extrapolated in syngenic 4T1/BALB/c *in vivo* mouse model of breast cancer. Because the model is syngenic in BALB/c mice, and employs animals that have functionally intact immune system, it allows for studying the role of immune system in tumor progression. To investigate role of mTORC2 in macrophage polarization we abrogated rictor expression in monocytes that had been reintroduced into mice. Mice treated with rictor knock down monocytes exhibited reduced tumor volume compared to mice receiving monocytes with control siRNA (Fig. 6). After cervical dislocation, the macrophages were isolated from ressected tumor mass. The macrophages from mice receiving rictor knock down monocytes exhibited diminished M2 macrophage polarization compared to rictor non-modulated monocyte in both untreated and OSM treated groups as evident by flowcytometry and immunofluroscence microscopy of isolated monocytes. Similar trend was observed in the mRNA levels of Arginase-1 and COX-2 (Fig. 7). Metastasis to distant organ such as liver, lung and bone was evaluated as a measurement of M2 macrophages assisted invasive potential. The control BALB/c mice that were not inoculated with 4T1 cells exhibited uniform tissue architecture of lung, liver and bone. As compared to vehicle control, OSM-treated 4T1/BALB/c mouse exhibited enhanced transformed cellular burden in lung, liver and bone where as mouse with reintroduced rictor abrogated macrophages had diminished metastatic foci in these organs in both OSM treated and non-treated animals (Fig. 8A–C). MicroCT analysis revealed formation of osteolytic lesions and loss of trabecular network in tibia exercised from tumor bearing mice as compared to Sham which were enhanced on OSM treatment. But mice reintroduce with rictor abrogated macrophages exhibited decreased number of osteolytic lesions and less loss of trabecular network (Fig. 9A and B).

4. Discussion

Our study demonstrates mTORC2 as a critical regulator of macrophage M2-polarization by hypoxic cancer cell secretome derived Oncostatin M. mTORC is key component of signaling networks that orchestrates various stress signals and regulate growth and homeostasis. This PI3KK family kinase nucleates at least 2 distinct multiprotein complex mTORC1 and mTORC2. mTORC2 plays a critical role in actin cytoskeleton reorganization and cell migration, protein synthesis and maturation, autophagy and metabolism. mTORC2 appears to be specifically involved in Th2 development as rictor null mice exhibits defective Th2 development. Byles et al. (2013) reported that constitutive mTORC1 activation renders macrophages refractory to IL-4 induced M2 polarization [16]. Although Festuccia et al. (2014) reported that rictor deletion induces M1 macrophage polarization in response to LPS [35]. While majority of reports indicate macrophages as being either M1 or M2 polarized subtype, studies conducted by Torroella-Kouri et al revealed that macrophages associated with D1-DMBA-3 mammary tumors are neither M1 nor M2 but, a poorly differentiated naive form of macrophages [36]. Although above studies suggest mTORC2 inactivation leading to M1 polarization; role of mTORC2 activation in M2 polarization of macrophages remains elusive. In view of this, the role of mTORC2 was investigated in M2 polarization of Macrophages particular to hypoxic cancer cell derived OSM. Our results revealed that both cell surface and functional markers specific to

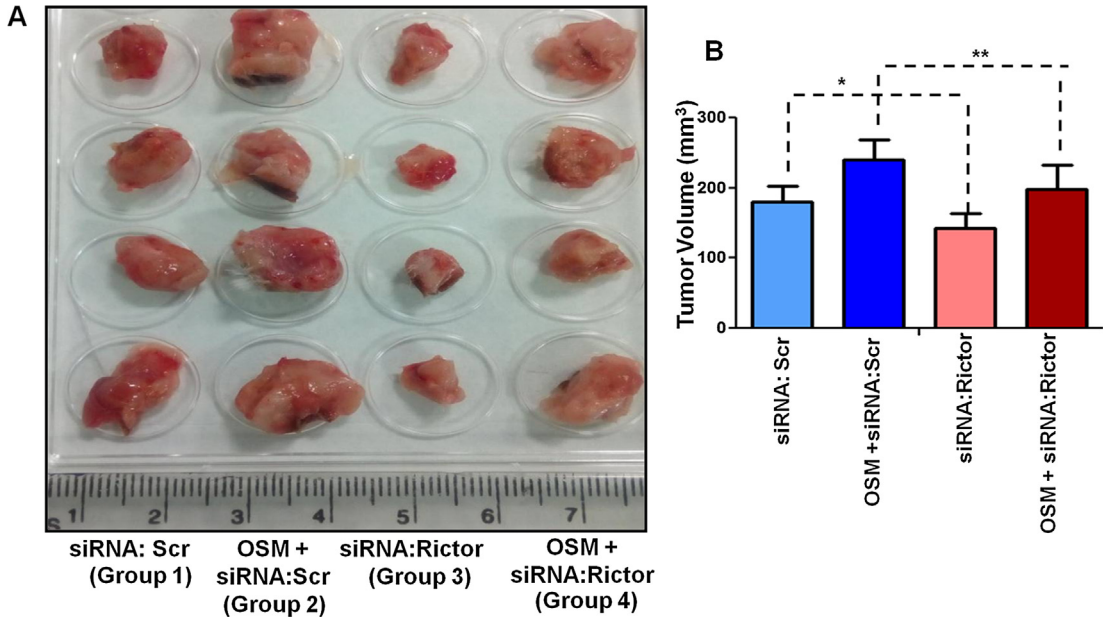

Fig. 6. *In vivo* myeloid specific rictor abrogation resulting in regression of 4T1 primary tumor. (A) Representative syngenic 4T1/BALB/c subcutaneous tumor specimens belonging to various groups described in suppl 12. (B) Quantification of tumor volumes (mm^3) of the indicated groups. $^{*}P < 0.05$, $^{**}P < 0.01$ and $^{***}P < 0.001$. (No. of animal per group (n) = 4).

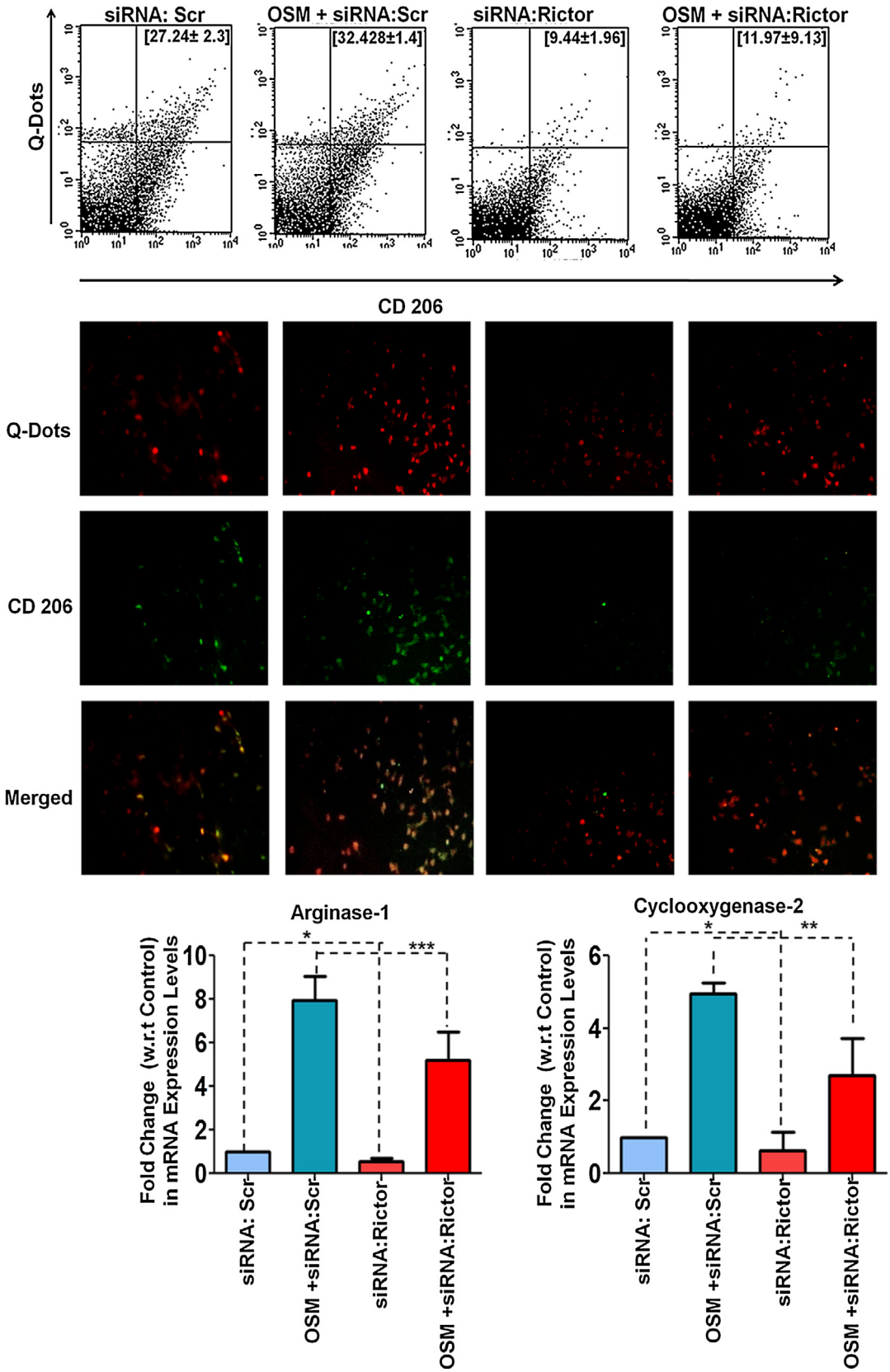

Fig. 7. *In vivo* myeloid specific rictor abrogation resulting in diminished recruitment and M2 polarization of tumor associated macrophages. (A) Comparison of M2 polarized population between scrambled and rictor silenced exogeneously reintroduced macrophage population. Extracted macrophages were labeled with Q-dots. Representative flowcytometry data and photomicrographs depicting M2 polarization of macrophages isolated from tumor using M2 surface markers anti-CD206 and RT-PCR analysis of M2 specific functional markers (Arg-1 and COX-2). Bars represent relative fold change in expression ± SEM. $^{*}P < 0.05$, $^{**}P < 0.01$ and $^{***}P < 0.001$. (No. of animal per group (n) = 4).

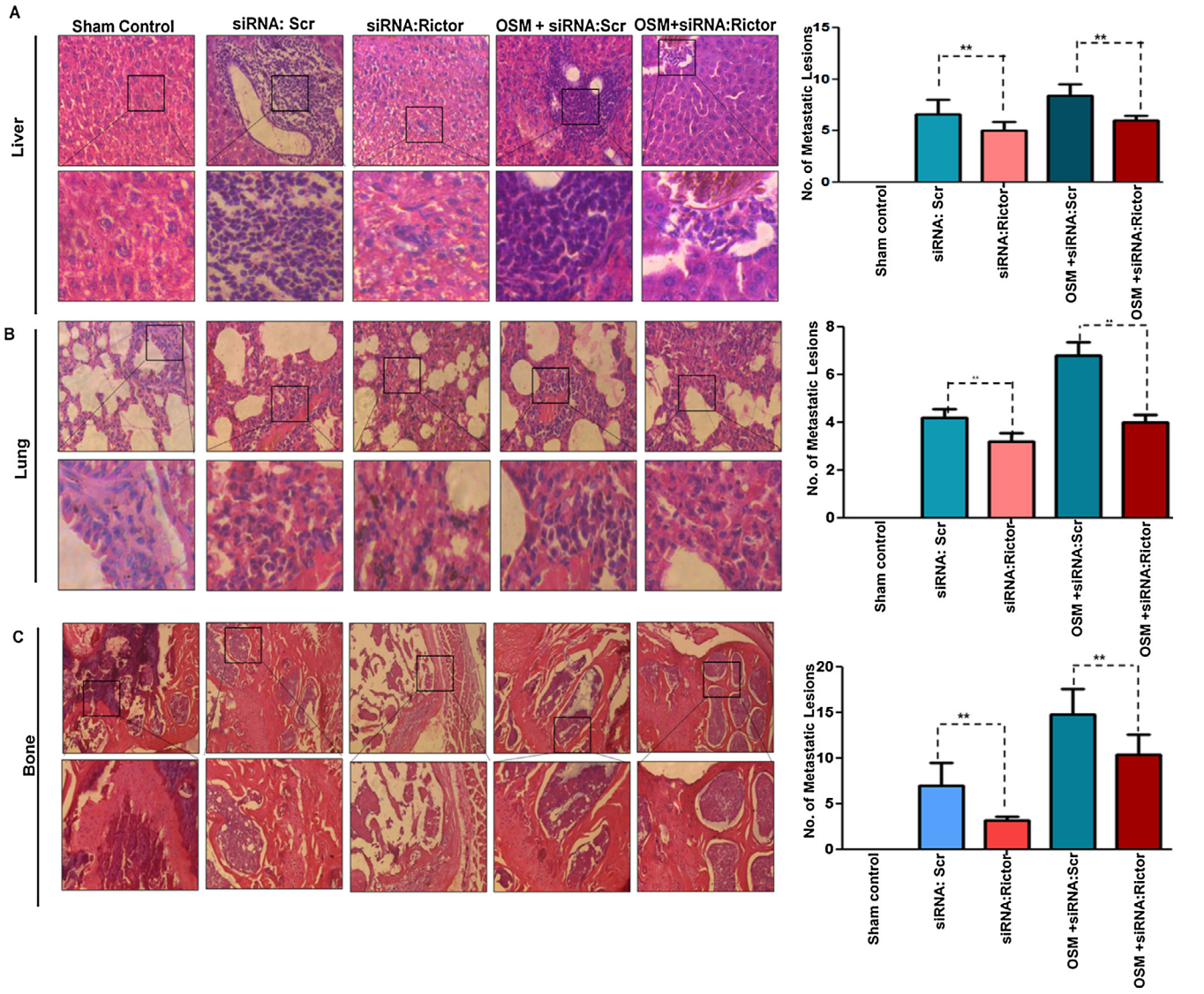

Fig. 8. *In vivo* myeloid specific rictor abrogation reduced cellular burden in lung and decreased metastatic lesions in liver and bone. (A) Hematoxylin and eosin stain, original magnification 20× upper and 40× lower of liver, lung (B) and bone (C) of sham control and various tumor groups as indicated in figure and corresponding quantification of no. of metastatic lesions. Experiment was done in duplicates thrice. Bars represent no. of metastatic lesions ± SEM. $^{*}P < 0.05$, $^{**}P < 0.01$ and $^{***}P < 0.001$ (No. of animal per group (n) = 4).

macrophage M2 macropahges were downregulated due to rictor deletion which is an approach to abrogate mTORC2 activation whereas its overexpression prompted macrophages to exhibit an enhanced expression of these markers.

After establishing the role of mTORC2 in OSM induced M2 polarization of macrophages, the downstream cascades involved were delineated. mTORC2 phosphorylates AGC kinases which includes Akt, PKC-α and SGK-1. While PKC-α activation pronouncedly requires mTORC2, Akt can be activated by various PDK1 kinase and non-receptor tyrosin kinases eg, ACK-1, ILK and MAPKAP2 [37,38]. Nonetheless, Akt1 is an established key mediator in signaling cascades involved in M2 polarization. SGK-1 is phosphorylated by mTORC2 at Ser422 but it still remains to be investigated whether indeed it is a mTORC2 dependent event, as its expression is elevated in rictor null cells. It has also been hypothesized to be regulated by rictor in an mTORC2 independent fashion [39]. Another effector substrate of mTORC2 is Akt [40]. Phosphorylation of HM site of Akt1 via mTORC2 has been shown to be elevated in numerous cancers [41]. Inhibition of Akt by Akt IV kinase inhibitor revealed that both hypoxic cancer cell CM and Oncostatin M induced macrophage M2 polarization was abrogated. Even mTORC2 activation via rictor upregulation could not prompt macrophages to acquire a M2 skewed phenotype when Akt was inhibited as evident by flowcytometric analysis and mRNA expression of Arg-1 and COX-2. PI3K is upstream activator of Akt, which is already established by the study as key mediator in OSM induced M2 polarization of macrophages [42]. Hence, further experiments were carried out to ascertain the definitive role of PI3K in OSM signaling cascade leading to M2 polarization. Interestingly, PI3K inhibition attenuated macrophage M2 polarization almost to the basal levels. This is indicated that OSM induced macrophages M2 polarization is precisely mediated by PI3K/Akt axis and mTORC2 activation could be an ancillary event. Gan et al. (2011) discovered evidence for direct activation of mTORC2 kinase activity by Phosphatidylinositol 3,4,5-Trisphosphate as PI3K facilitates (PtdIns $(3,4,5)P_3$) which non-specifically activates various kinases including mTORC2 [34]. To assess this, exogeneous addition of (PtdIns$(3,4,5)P_3$) restored OSM induced M2 polarization of macrophages in which PI3K was inhibited. However, addition of (PtdIns$(3,4,5)P_3$) could not overcome inhibitory effect of abrogation of mTORC2. Hence, mTORC2 can be considered as vital determinant for macrophage M2 polarization.

Akt exists in three isoforms i.e Akt1, Akt2 and Akt3. Akt1 was

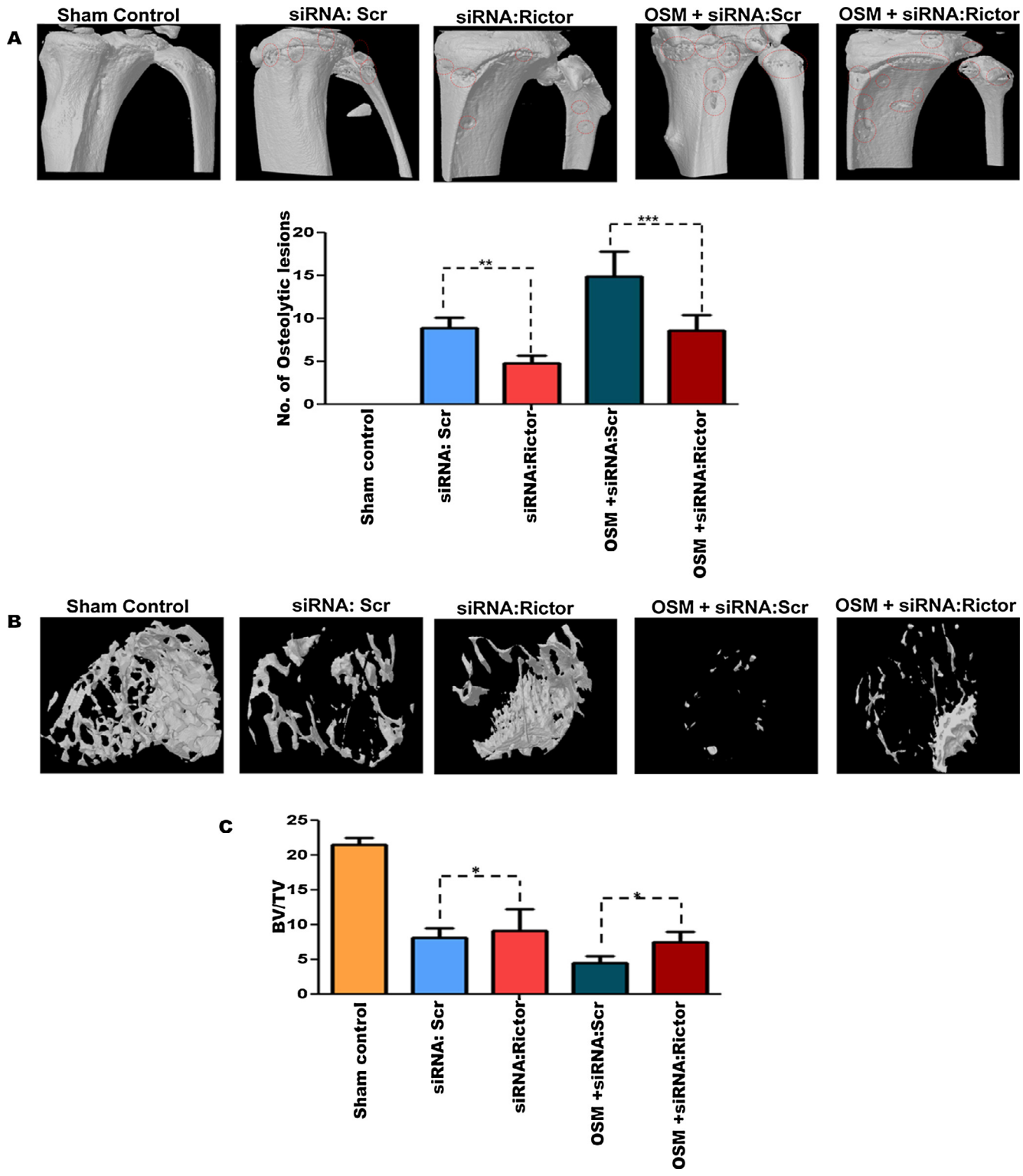

Fig. 9. *In vivo* myeloid specific rictor abrogation reduced formation of osteolytic lesions and loss of trabecular network. (A) Representative 3D reconstruction of tibia showing osteolytic lesions (Red circle) network in sham control and various tumor groups as indicated in figure and its corresponding quantification. Bars represent no. of osteolytic lesions ± SEM. $^{*}P < 0.05$, $^{**}P < 0.01$ and $^{***}P < 0.001$. (B) Representative 2D cross section of tibia showing loss of trabecular network in sham control and various tumor groups as indicated in figure. (C) Quantification of BV/TV (Trabecular volume) of sham control and various tumor groups as indicated in figure. $^{*}P < 0.05$, $^{**}P < 0.01$ and $^{***}P < 0.001$. (No. of animal per group (n) = 4).

originally identified as the oncogene in retrovirus. Akt1 is involved in cellular survival pathways, inhibiting apoptosis and inducing protein synthesis pathways. Its activation has a role in skeletal muscle hypertrophy and general tissue growth. Akt1 deleted mouse models exhibit growth retardation and promotes cell survival [43]. Akt2 is a important signaling molecule in insulin signaling and induces glucose uptake. Mouse null for Akt2 but normal for Akt1 are smaller in size and display a diabetic phenotype [44]. Akt3 has been reported to have a limited tissue distribution and most commonly exist in brain. Akt3 null mice have normal growth and metabolism but have small brains [45]. Arranz

et al., reported that Akt1 and Akt2 differentially regulate macrophage polarization and ablation of Akt1 gives rise to M1 phenotype [29]. In view of this, attempt was made for evaluating which isoform could be involved in Oncostatin M induced macrophage M2 polarization. Role of Akt1 isoform was unraveled by using Akt dominant negative gene construct (pHRIG-Akt1DN). The Akt1DN gene construct is an Akt gene where a point mutation in the 179th amino acid from the N terminal converts a lysine to a methionine. This mutated form of the Akt1 protein can still be phosphorylated at the Ser473 site but loses its ability to relay signals to downstream effectors factors [46]. Flowcytometric analysis and immunocytochemistry ascertained that inhibition of Akt1 abrogated the effect of OSM induced M2 polarization. Hence, it was confirmed that OSM induced macrophage M2 polarization is mediated by mTORC2 through downstream activation of Akt1.

To ascertain physiological relevance of these observations, the findings were validated using *in vivo* 4T1/BALB/c mouse orthotropic model of breast cancer. Mouse models have been extensively employed in immunological experiments and they reflect many aspects similar to human immunology [47]. Although there do exist immunological differences particularly pertaining to cytokine biology [48]. For instance, humans are sensitive to LPS in nanograms of dose whereas mice require LPS in milligrams to induce cytokine release [49,50]. Mouse serum when added to human mononuclear cells diminishes release of cytokines [51]. However, effect of Oncostatin M is found to be similar in both mouse and human macrophages. But there does exists a difference between interaction of human OSM (hOSM) and mouse OSM (mOSM) with their receptors. hOSM binds to both LIFR (gp130/LIFRβ) and OSMR (gp130/OSMRβ) receptor complexes. Whereas mOSM interact with only gp130/OSMRβ receptor complex [52]. Oncostatin M induces M2 macrophage phenotype in mouse models of diabetes and obesity [53,54]. The endogenous monocytes of these mice were depleted with a monocyte depletor ($GdCl_3$) to synchronize the recruitment of monocytes which were exogeneously reintroduced after experimental manipulations. Our results revealed that abrogation of mTORC2 in monocytes hindered recruitment of macrophages in both control as well as Oncostatin M treated groups as reported by us earlier. The polarization of TAMs towards M2 phenotype was also decreased in mTORC2 inhibited macrophages. These findings highlighted the critical involvement of mTORC2 signaling in M2 polarization of TAMs. We further investigated the metastasis of breast tumor to distant organs like liver, lung and bone. The results demonstrated that decreases in formation of metastatic lesions in these organs and restored trabecular bone network in mice which received mTORC2 abrogated monocytes.

Hence, this study paves way for development of specific mTORC2 inhibitors as a strategy to counteract M2 polarization and its associated tumor progression and metastasis either alone or in combination with established anti cancer therapeutics. Further extensive clinical studies are required to translate these findings into an effective therapeutic approach; nonetheless, our study establishes specific mTORC2 inhibitors as a potential target for devising newer anti-cancer immunotherapeutics.

Acknowledgements

Authors thank Director CSIR-CDRI for infrastructure/facility support, Division of Sophisticated Analytical Instruments Facility (SAIF) for Flowcytometric Analysis and Tissue and cell culture unit for providing cell lines. This work was supported by grants from CSIR-Network Project-BSC0103 and CSIR fellowship. The CDRI communication number for this manuscript is 9643.

Authors contribution

Conception and design: Smrati Bhadauria and Richa Shrivastava.

Development of methodology: Richa Shrivastava, Varsha Singh and Showkat Ahmad Malik.

Acquisition of data: Richa Shrivastava, Mohammad Asif, Subhashis Pal, Geet Kumar Nagar, Khemraj Singh Baghel, Mehraj lone.

Analysis and interpretation of data: Smrati Bhadauria, Brij Nath Tewari, Naibedya Chattopadhyay.

Writing, review and/or revision of the manuscript: Smrati Bhadauria, Richa Shrivastava, Mohammad Asif and Parul Dubey.

Conflict of interest

The authors declare no potential conflicts of interest exist.

Appendix A. Supplementary material

Supplementary data associated with this article can be found, in the online version, at https://doi.org/10.1016/j.cyto.2018.03.032.

References

[1] A. Sica, et al., Tumour-associated macrophages are a distinct M2 polarised population promoting tumour progression: potential targets of anti-cancer therapy, Eur. J. Cancer 42 (6) (2006) 717–727.
[2] S. Sousa, et al., Human breast cancer cells educate macrophages toward the M2 activation status, Breast Cancer Res. 17 (2015) 101.
[3] L. Bingle, N.J. Brown, C.E. Lewis, The role of tumour-associated macrophages in tumour progression: implications for new anticancer therapies, J. Pathol. 196 (3) (2002) 254–265.
[4] S. Gordon, P.R. Taylor, Monocyte and macrophage heterogeneity, Nat. Rev. Immunol. 5 (12) (2005) 953–964.
[5] T. Lawrence, G. Natoli, Transcriptional regulation of macrophage polarization: enabling diversity with identity, Nat. Rev. Immunol. 11 (11) (2011) 750–761.
[6] A. Mantovani, et al., The chemokine system in diverse forms of macrophage activation and polarization, Trends Immunol. 25 (12) (2004) 677–686.
[7] F.O. Martinez, S. Gordon, The M1 and M2 paradigm of macrophage activation: time for reassessment, F1000Prime Rep. 6 (2014) 13.
[8] S.K. Biswas, A. Sica, C.E. Lewis, Plasticity of macrophage function during tumor progression: regulation by distinct molecular mechanisms, J. Immunol. 180 (4) (2008) 2011–2017.
[9] S. Ohno, et al., Correlation of histological localization of tumor-associated macrophages with clinicopathological features in endometrial cancer, Anticancer Res. 24 (5C) (2004) 3335–3342.
[10] R.D. Leek, et al., Necrosis correlates with high vascular density and focal macrophage infiltration in invasive carcinoma of the breast, Br. J. Cancer 79 (5–6) (1999) 991–995.
[11] R.D. Leek, et al., Association of tumour necrosis factor alpha and its receptors with thymidine phosphorylase expression in invasive breast carcinoma, Br. J. Cancer 77 (12) (1998) 2246–2251.
[12] J.L. Burton, N. Oakley, J.B. Anderson, Recent advances in the histopathology and molecular biology of prostate cancer, BJU Int. 85 (1) (2000) 87–94.
[13] R.P. Negus, et al., Quantitative assessment of the leukocyte infiltrate in ovarian cancer and its relationship to the expression of C-C chemokines, Am. J. Pathol. 150 (5) (1997) 1723–1734.
[14] C. Tripathi, et al., Macrophages are recruited to hypoxic tumor areas and acquire a pro-angiogenic M2-polarized phenotype via hypoxic cancer cell derived cytokines Oncostatin M and Eotaxin, Oncotarget 5 (14) (2015) 5350–5368.
[15] M. Tanaka, A. Miyajima, Oncostatin M, a multifunctional cytokine, Rev. Physiol. Biochem. Pharmacol. 149 (2003) 39–52.
[16] G. Bilbe, et al., PCR phenotyping of cytokines, growth factors and their receptors and bone matrix proteins in human osteoblast-like cell lines, Bone 19 (5) (1996) 437–445.
[17] C.L. Jorcyk, R.G. Holzer, R.E. Ryan, Oncostatin M induces cell detachment and enhances the metastatic capacity of T-47D human breast carcinoma cells, Cytokine 33 (6) (2006) 323–336.
[18] M.B. Crichton, et al., Expression of transcripts of interleukin-6 and related cytokines by human breast tumors, breast cancer cells, and adipose stromal cells, Mol. Cell. Endocrinol. 118 (1–2) (1996) 215–220.
[19] M.M. Queen, et al., Breast cancer cells stimulate neutrophils to produce oncostatin M: potential implications for tumor progression, Cancer Res. 65 (19) (2005) 8896–8904.
[20] G.M. Argast, et al., Cooperative signaling between oncostatin M, hepatocyte growth factor and transforming growth factor-beta enhances epithelial to mesenchymal transition in lung and pancreatic tumor models, Cells Tissues Organs 193 (1–2) (2011) 114–132.
[21] R.G. Holzer, et al., Oncostatin M stimulates the detachment of a reservoir of invasive mammary carcinoma cells: role of cyclooxygenase-2, Clin. Exp. Metastasis 21 (2) (2004) 167–176.
[22] C. Bolin, et al., Oncostatin m promotes mammary tumor metastasis to bone and osteolytic bone degradation, Genes Cancer 3 (2) (2012) 117–130.
[23] D. Duluc, et al., Tumor-associated leukemia inhibitory factor and IL-6 skew monocyte differentiation into tumor-associated macrophage-like cells, Blood 110 (13) (2007) 4319–4330.

[24] N.R. West, J.I. Murray, P.H. Watson, Oncostatin-M promotes phenotypic changes associated with mesenchymal and stem cell-like differentiation in breast cancer, Oncogene 33 (12) (2014) 1485–1494.
[25] M. Daigneault, et al., The identification of markers of macrophage differentiation in PMA-stimulated THP-1 cells and monocyte-derived macrophages, PLoS One 5 (1) (2010) e8668.
[26] O.H. Lowry, et al., Protein measurement with the Folin phenol reagent, J. Biol. Chem. 193 (1) (1951) 265–275.
[27] M.W. Pfaffl, A new mathematical model for relative quantification in real-time RT-PCR, Nucl. Acids Res. 29 (9) (2001) e45.
[28] W. Chen, et al., Macrophage-induced tumor angiogenesis is regulated by the TSC2-mTOR pathway, Cancer Res. 72 (6) (2012) 1363–1372.
[29] A. Arranz, et al., Akt1 and Akt2 protein kinases differentially contribute to macrophage polarization, Proc. Natl. Acad. Sci. USA 109 (24) (2012) 9517–9522.
[30] D.W. Lamming, et al., Depletion of Rictor, an essential protein component of mTORC2, decreases male lifespan, Aging Cell 13 (5) (2014) 911–917.
[31] Y.X. Zhang, et al., Effect of protein kinase C alpha, caspase-3, and survivin on apoptosis of oral cancer cells induced by staurosporine, Acta Pharmacol. Sin. 26 (11) (2005) 1365–1372.
[32] C. Courage, J. Budworth, A. Gescher, Comparison of ability of protein kinase C inhibitors to arrest cell growth and to alter cellular protein kinase C localisation, Br. J. Cancer 71 (4) (1995) 697–704.
[33] J. Lee, et al., Genetic reconstruction of mouse spermatogonial stem cell self-renewal in vitro by Ras-cyclin D2 activation, Cell Stem Cell 5 (1) (2009) 76–86.
[34] X. Gan, et al., Evidence for direct activation of mTORC2 kinase activity by phosphatidylinositol 3,4,5-trisphosphate, J. Biol. Chem. 286 (13) (2011) 10998–11002..
[35] W.T. Festuccia, et al., Myeloid-specific Rictor deletion induces M1 macrophage polarization and potentiates in vivo pro-inflammatory response to lipopolysaccharide, PLoS One 9 (4) (2014) e95432.
[36] M. Torroella-Kouri, et al., Identification of a subpopulation of macrophages in mammary tumor-bearing mice that are neither M1 nor M2 and are less differentiated, Cancer Res. 69 (11) (2009) 4800–4809.
[37] T. Ikenoue, et al., Essential function of TORC2 in PKC and Akt turn motif phosphorylation, maturation and signalling, EMBO J. 27 (14) (2008) 1919–1931.
[38] J.T. Stuenaes, et al., Beta-adrenoceptor stimulation potentiates insulin-stimulated PKB phosphorylation in rat cardiomyocytes via cAMP and PKA, Br. J. Pharmacol. 160 (1) (2010) 116–129.
[39] D. Gao, et al., Rictor forms a complex with Cullin-1 to promote SGK1 ubiquitination and destruction, Mol. Cell 39 (5) (2010) 797–808.
[40] D.D. Sarbassov, et al., Phosphorylation and regulation of Akt/PKB by the rictor-mTOR complex, Science 307 (5712) (2005) 1098–1101.
[41] D.A. Guertin, et al., mTOR complex 2 is required for the development of prostate cancer induced by Pten loss in mice, Cancer Cell 15 (2) (2009) 148–159.
[42] D.C. Smyth, et al., Oncostatin M induction of eotaxin-1 expression requires the convergence of PI3'K and ERK1/2 MAPK signal transduction pathways, Cell Signal 20 (6) (2008) 1142–1150.
[43] H. Cho, et al., Akt1/PKBalpha is required for normal growth but dispensable for maintenance of glucose homeostasis in mice, J Biol Chem 276 (42) (2001) 38349–38352.
[44] R.S. Garofalo, et al., Severe diabetes, age-dependent loss of adipose tissue, and mild growth deficiency in mice lacking Akt2/PKB beta, J. Clin. Invest. 112 (2) (2003) 197–208.
[45] R.M. Easton, et al., Role for Akt3/protein kinase Bgamma in attainment of normal brain size, Mol. Cell. Biol. 25 (5) (2005) 1869–1878.
[46] R. Xie, et al., Akt isoforms differentially protect against stroke-induced neuronal injury by regulating mTOR activities, J. Cereb. Blood Flow Metab. 33 (12) (2013) 1875–1885.
[47] J. Mestas, C.C. Hughes, Of mice and not men: differences between mouse and human immunology, J. Immunol. 172 (5) (2004) 2731–2738.
[48] J. Zschaler, D. Schlorke, J. Arnhold, Differences in innate immune response between man and mouse, Crit. Rev. Immunol. 34 (5) (2014) 433–454.
[49] T. van der Poll, et al., Interleukin-1 receptor blockade does not affect endotoxin-induced changes in plasma thyroid hormone and thyrotropin concentrations in man, J. Clin. Endocrinol. Metab. 80 (4) (1995) 1341–1346.
[50] K. Reynolds, et al., Pretreatment with troglitazone decreases lethality during endotoxemia in mice, J Endotoxin Res 8 (4) (2002) 307–314.
[51] H.S. Warren, et al., Resilience to bacterial infection: difference between species could be due to proteins in serum, J. Infect. Dis. 201 (2) (2010) 223–232.
[52] H.M. Hermanns, Oncostatin M and interleukin-31: Cytokines, receptors, signal transduction and physiology, Cytokine Growth Factor Rev. 26 (5) (2015) 545–558.
[53] S. Lauber, et al., Novel function of Oncostatin M as a potent tumour-promoting agent in lung, Int. J. Cancer 136 (4) (2015) 831–843.
[54] T. Komori, et al., Lack of oncostatin M receptor beta leads to adipose tissue inflammation and insulin resistance by switching macrophage phenotype, J. Biol. Chem. 288 (30) (2013) 21861–21875.